Geometric Clustering of Polsar Data Using the Polar Decomposition

Madalina Ciuca, Gabriel Vasile, Marco Congedo

GEOMETRIC CLUSTERING OF POLSAR DATA USING THE POLAR DECOMPOSITION

Madalina Ciuca[⋆§] *Gabriel Vasile*[⋆] *Marco Congedo*[⋆]
[⋆] Univ. Grenoble Alpes, CNRS / Grenoble INP, Grenoble, France
[§] University POLITEHNICA of Bucharest, Bucharest, Romania

ABSTRACT

This paper presents a new method for geometrical PolSAR clustering based on two fundamental concepts: the polar decomposition of scattering matrices and the Riemannian geometry of their Hermitian factors. The method is applied in a cohesive manner for both coherent and incoherent scatterers. A qualitative comparison is performed with two clustering algorithms based on the covariance framework and two different evaluation metrics: one stochastic – Wishart and one geometric – cosine geodesic. Results on a real dataset show that the final classification better preserves small details and the original texture information in the PolSAR image. In this regard, an improved separation is observed, for example, for certain vegetation fields.

Index Terms— PolSAR, polar decomposition, scattering matrix, Hermitian, unitary, Riemannian manifold, AIRM, clustering, classification, k-means.

1. INTRODUCTION

Polarimetric Synthetic Aperture Radar (PolSAR) is based on the coherent measurement of microwave scattering diversity in two orthogonal polarization bases. As in any data analysis field, both supervised and unsupervised classification methods have been used with this complex multidimensional data. Whereas supervised algorithms use a wide variety of input features, the unsupervised ones are consistent in this regard. Coherent methods use the scattering matrix/vector and the incoherent ones, by far the largest and befitting category in practical applications, use the covariance/coherency matrices.

Within unsupervised methods, the clustering-based subfield is undeniably popular, amidst which the unsupervised Wishart [1] (and derivations) have reached cross-domain applicability (with the best results when used for homogeneous, complex-Gaussian distributed data). Because of its versatility and algorithmic similarity to the proposed technique, we use the method as benchmark.

The remainder of this paper is organised as follows. Section 2 briefly introduces the main theoretical aspects and offers details on the proposed algorithm and Section 3 presents results of real data evaluation. Conclusions are given in Section 4.

2. POLAR DECOMPOSITION, HERMITIAN FACTORS AND THE RIEMANNIAN MANIFOLD

2.1. Polar decomposition

The polar decomposition can be used to decompose the PolSAR scattering matrix into a product of two factors [2]:

$$\mathbf{S} = \mathbf{U}\mathbf{H} \tag{1}$$

The first term is *unitary* ($\mathbf{U}$, $\mathbf{U}\mathbf{U}^H = \mathbf{I}$, $\mathbf{U} \in \mathbb{C}^{2\times2}$) and the second is *Hermitian* ($\mathbf{H}$, $\mathbf{H}^H = \mathbf{H}$, $\mathbf{H} \in \mathbb{C}^{2\times2}$). By convention, (1) is known as the right polar decomposition and is the form used in this paper. This decomposition is the matrix equivalent of the well-known polar form, which writes every non-zero complex number $s = s_1 + js_2$, $s \in \mathbb{C}$, as the product of a modulus and a phase element: $s = |s| \cdot e^{j\theta}$, $\theta \in [-\pi, \pi]$. Analogously, the $\mathbf{H}$ and $\mathbf{U}$ factors of the decomposition represents a linear "boost" and a rotation, respectively [2].

The unitary matrices are the complex counterpart of orthogonal matrices. They preserve lengths and many distance functions are unitary-invariant. It is more common to refer to the orthogonal matrices as to (real) rotations [1]. However, a 2×2 unitary matrix can be expressed as the product between a diagonal phase matrix and a special $SU(2)$ matrix, or equivalently, as the product of two phase matrices and one real rotation [3]. That is, the action of a unitary matrix is that of both a rotation and of phase changes. As the modulus of a complex number allows to obtain a quantity's phase-invariant amplitude and the discharge of a real rotation in PolSAR gives a rotation-invariant element, we argue that the $\mathbf{H}$-factor from the polar decomposition can be seen as both phase and rotation invariant. Based on this desirable property of the Hermitian $\mathbf{H}$-factors, we propose a geometric unsupervised clustering which exploits their Riemannian geometry.

2.2. Hermitian factors and Riemannian manifold

The positive definite matrices, as the $\mathbf{H}$-factors, are naturally embedded in a non-linear, smooth, differentiable, Riemannian manifold. In this space, the shortest path connecting any

[1]

	real rotation	complex rotation
	$\begin{bmatrix}\cos\theta & -\sin\theta \\ \sin\theta & \cos\theta\end{bmatrix}$	$\begin{bmatrix}\cos\theta & -\sin\theta e^{-j\varphi} \\ \sin\theta e^{j\varphi} & \cos\theta\end{bmatrix}$

two points is no longer a straight line (as in the Euclidean space), but a path which follows the curvature of the space and known as a *geodesic*. The most commonly employed metrics in the Riemannian manifold of positive Hermitian matrices are the affine invariant Riemann metric (AIRM) and the Log-Euclidean metric. They both allow the definition of a distance function in closed-form.

These two geometric metrics have been used in previous PolSAR applications operating in the Riemannian embedding of coherency/covariance matrices [4, 5]. Another metric used in PolSAR is the angular geodesic, which can be seen as an approximation of the true geodesic, but only when restricting the shape of the Riemannian manifold to that of a unit sphere [6].

For any two positive definite matrices $\mathbf{H_1}$ and $\mathbf{H_2}$, AIRM gives the minimum distance along the Riemannian geodesic[2]

$$d(\mathbf{H_1}, \mathbf{H_2}) = ||\operatorname{Log}(\mathbf{H_1}^{-1/2}\mathbf{H_2}\mathbf{H_1}^{-1/2})||_F. \quad (2)$$

For m positive definite matrices $\{\mathbf{H_1}, \mathbf{H_2}, \ldots, \mathbf{H_m}\}$, $m > 2$, the Riemannian barycenter, i.e., the geometric center of mass (known also as the geometric mean) [7], is a point $\mathbf{H_0}$ which attains the minimum dispersion, i.e.,

$$\arg\min_{\mathbf{H_0}} \sum_{i=1}^{m} d(\mathbf{H_0}, \mathbf{H_i})^2. \quad (3)$$

While there is no closed-form solution for the minimization problem in (3), it was shown that the minimum always exists and is unique [8]. Moreover, when the dispersion is not excessive the minimizer can be attained with probability 1 by a simple gradient descent algorithm [4].

2.3. Proposed method

The proposed method is presented in pseudo-code (Algorithm 1).

Algorithm 1: Riemannian k-means using polar $\mathbf{H}$-factors.

Input: Full-polarimetric data in scattering matrix format, $\mathbf{S}$.

1 Decompose $\mathbf{S}$ via the polar decomposition and obtain the $\mathbf{H}$-factors.

2 Evaluate the presence of coherent scatterers (method: 98^{th} percentile criterion by Lee et al. [9], evaluation: 3×3 boxcar). Compose binary map of incoherent/coherent scattering positions.

3 Mask-out positions of coherent scatterers and compute for each remaining position the $\mathbf{H}$-factor barycenter. (Evaluation method: square, sliding neighbourhood).

4 Apply the geometrical k-means clustering method [3]. For positions of coherent scatterers, their Hermitian $\mathbf{H}$-factor is used. Random initialization is applied for class centres and the intra/inter-cluster evaluation is based on the AIRM metric.

5 Stop algorithm when the predefined threshold (accuracy/nr. of runs) is reached.

3. EXPERIMENTAL RESULTS

3.1. PolSAR Dataset

The experimental study uses a PolSAR dataset acquired by the SAR ElectroMagnetic Institute Synthetic Aperture Radar (EMISAR) instrument over the Foulum test site [10]. It shows a mixture of vegetation areas (different crop fields, forest), small urban areas and a lake/water reservoir (Pauli composite in Fig. 1a).

The EMISAR Foulum full-polarimetric dataset is well-known in the PolSAR community and a number of publications show incomplete descriptions of the area's perennial/permanent vegetation content, as for example [11–13]. Due to its richness of natural elements it has been used for vegetation studies [12], statistical assessments in homogeneous/inhomogeneous regions [11] and others. Recently, incomplete ground truth representations have been proposed for evaluation of machine learning architectures and we display one such example in Fig. 1(b) [14].

3.2. Clustering comparison

For illustration purposes, Fig. 1(c) shows the amplitude in the $h_{1,1}$ channel of the Hermitian barycenters. A gray scale display of the span in the original image will give similar results, which can even be motivated mathematically.

The remaining subfigures display three clustering results. Fig. 1(d) is obtained applying the proposed, Riemannian k-means method, while Fig. 1(e) is the result of the classical Wishart method. For Fig. 1(f), a different implementation is proposed, based on the same k-means framework/initialization as with Wishart, but using the cosine geodesic distance as inter/intra-cluster metric. The main differences between the three implementations are summarized in Table 1.

Comparing the three results, the large scale features seem to be well identified by all methods, while the texture information is better preserved when using the two geometrical distances (Figs. 1d & f). However, the proposed Riemannian k-means seems to exhibits better accuracy, as it is able to

[2]Notations: Log = matrix logarithm. $\|\cdot\|_F$ = Frobenius norm.

[3]Note: From a computer science perspective, the better name to be used is k-medoids. It refers to a clustering technique, similar to k-means, apart from the centroid computation. While in k-means the class centroid may be different from the existing elements of a class (as a result of averaging), the metric criteria for k-medoids selects the center/centroid from inside a class' elements. Nonetheless, we stick to the more common name in PolSAR.

Table 1: Differences in clustering algorithms implementation.

Method	Input matrices	Initialization	Metric (intra/inter-class)
Riemannian k-means[3]	$\mathbf{S}$	random	AIRM (2)
Wishart	$\mathbf{C}$	H-α	$d(\mathbf{C_1}, \mathbf{C_2}) = \ln\lvert\mathbf{C_2}\rvert + \mathrm{tr}(\mathbf{C_2}^{-1}\mathbf{C_1})$, [1]
Cosine GD k-means[3]	$\mathbf{C}$	H-α	$d(\mathbf{C_1}, \mathbf{C_2}) = \cos^{-1}\left(\frac{\mathrm{tr}(\mathbf{C_1}^H\mathbf{C_2})}{\sqrt{\mathrm{tr}(\mathbf{C_1}^H\mathbf{C_1})}\sqrt{\mathrm{tr}(\mathbf{C_2}^H\mathbf{C_2})}}\right)$, [6]

discriminate crop fields which are not retrieved by the other two methods. For example, the beet and winter wheat fields, from the ground truth (yellow and dark blue, respectively), are correctly separated as distinct classes, both when in close proximity and farther apart in the image.

4. CONCLUSION

This paper focuses on the use of the Riemannian framework throughout all stages of a PolSAR clustering application. The use of the polar decomposition allows both a reduction in dimensions and phase/rotation invariance of the input features. Intrinsically, the proposed framework represents a shift in the current PolSAR computation paradigm.

From an algebraic perspective, the true informational space for polarimetric measurements through the 2×2 scattering matrix is $\mathbb{C}^{2\times2}$, while the extension to covariance Hermitian $\mathbb{C}^{3\times3}$ is only through second order statistics. That is why, instead of statistically averaging the scattering vectors (as for covariance/coherency matrix estimation), a geometrical local mean (i.e., barycenter) is computed based on a geodesic distance associated to the manifold. In other words, the algorithm does not modify the algebraic and geometric structure of the input features, rather it takes advantage of them.

5. REFERENCES

[1] J.-S. Lee, M. Grunes, T. Ainsworth, L.-J. Du, D. Schuler, and S. Cloude, "Unsupervised classification using polarimetric decomposition and the complex Wishart classifier," *IEEE Trans. Geosci. Remote Sens.*, vol. 37, no. 5, pp. 2249–2258, 1999.

[2] J.-C. Souyris and C. Tison, "Polarimetric analysis of bistatic SAR images from polar decomposition: A quaternion approach," *IEEE Trans. Geosci. Remote Sens.*, vol. 45, no. 9, pp. 2701–2714, 2007.

[3] D. P., "Factorization of unitary matrices," *Journal of Physics A: Mathematical and General*, vol. 36, no. 11, pp. 2781, 2003.

[4] P. Formont, J.-P. Ovarlez, and P. Frédéric, *On the Use of Matrix Information Geometry for Polarimetric SAR Image Classification*, Springer Berlin Heidelberg, Berlin, Heidelberg, 2013.

[5] N. Zhong, W. Yang, A. Cherian, X. Yang, G.-S. Xia, and M. Liao, "Unsupervised classification of polarimetric SAR images via Riemannian sparse coding," *IEEE Trans. Geosci. Remote Sens.*, vol. 55, no. 9, pp. 5381–5390, 2017.

[6] D. Ratha, A. Bhattacharya, and A. C. Frery, "Unsupervised classification of PolSAR data using a scattering similarity measure derived from a geodesic distance," *IEEE Geosci. Remote Sens. Lett.*, vol. 15, no. 1, pp. 151–155, 2018.

[7] R. Bhatia, *The Riemannian Mean of Positive Matrices*, pp. 35–51, Springer Berlin Heidelberg, Berlin, Heidelberg, 2013.

[8] A. Barachant, S. Bonnet, M. Congedo, and C. Jutten, "Multiclass brain–computer interface classification by Riemannian geometry," *IEEE Trans. Biomed. Eng.*, vol. 59, no. 4, pp. 920–928, 2012.

[9] J.-S. Lee, T. L. Ainsworth, Y. Wang, and K.-S. Chen, "Polarimetric SAR speckle filtering and the extended Sigma filter," *IEEE Trans. Geosci. Remote Sens.*, vol. 53, no. 3, pp. 1150–1160, 2015.

[10] N. Skou, J. Granholm, K. Woelders, J. Rohde, J. Dall, and E. Christensen, "A high resolution polarimetric L-band SAR-Design and results," in *International Geoscience and Remote Sensing Symposium, IGARSS '95*, 1995, vol. 3, pp. 1779–1782 vol.3.

[11] K. Conradsen, A. Nielsen, J. Schou, and H. Skriver, "A test statistic in the complex Wishart distribution and its application to change detection in polarimetric SAR data," *IEEE Trans. Geosci. Remote Sens.*, vol. 41, no. 1, pp. 4–19, 2003.

[12] H. Skriver, J. Dall, L. Ferro-Famil, T. Toan, P. Lumsdon, R. Moshammer, E. Pottier, and S. Queguan, "Agriculture classification using PolSAR data," in *POLINSAR 2005*, Italy, 2005, pp. 32–37.

[13] A. P. Doulgeris and T. Eltoft, "Scale mixture of gaussian modelling of polarimetric SAR data," *Journal on Advances in Signal Processing*, vol. 1, pp. 1687–6180, 2009.

[14] H. Dong, L. Zhang, and B. Zou, "PolSAR image classification with lightweight 3D convolutional networks," *Remote Sensing*, vol. 12, no. 3, 2020.

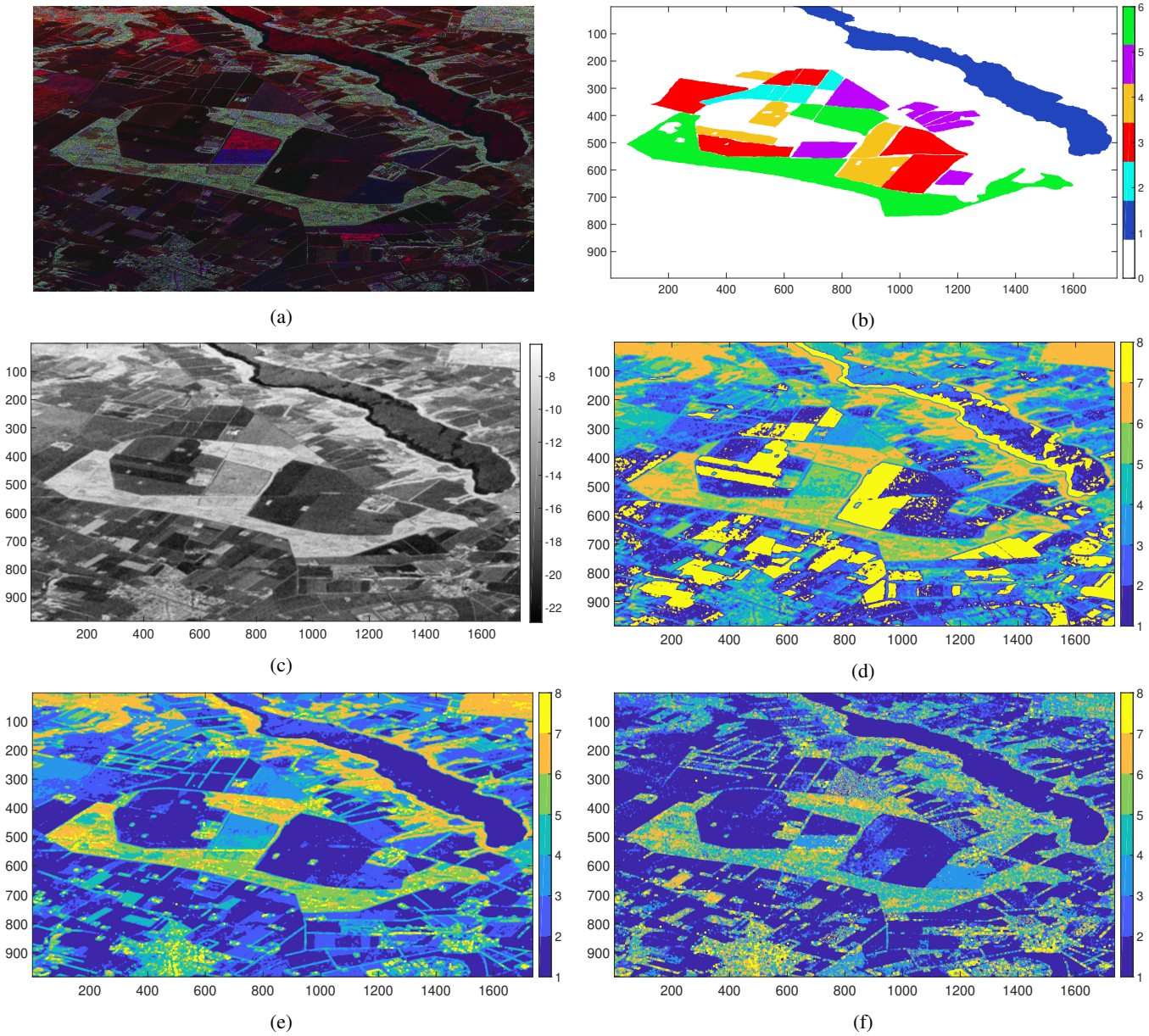

Fig. 1: Foulum Dataset. (a) Pauli decomposition (R: $\frac{S_{hh}+S_{vv}}{2}$, G: $\frac{S_{hv}+S_{vh}}{2}$, B: $\frac{S_{hh}-S_{vv}}{2}$). (b) Incomplete ground truth (as in [14]). Legend: blue - water; green - forest; cyan - peas; magenta - winter rape; red - winter wheat; yellow - beet. (c) $\mathbf{H}$ barycenters ($h_{1,1}$, amplitude, [dB]). (d) $\mathbf{H}$-factors Riemannian k-means clustering. (e) Wishart clustering. (f) k-means clustering with cosine geodesic distance.